Shape-Controlled Nanoparticles

DOI: 10.1002/anie.200603068

Morphological Control of Catalytically Active Platinum Nanocrystals**

*Hyunjoo Lee, Susan E. Habas, Sasha Kweskin, Derek Butcher, Gabor A. Somorjai, and Peidong Yang**

Colloidal metallic nanocrystals have been explored for catalytic applications, including fine chemicals synthesis,[1] fuel-cell technology,[2] hydrogen production,[3] and gas sensing.[4] The catalytic activity of a metallic catalyst depends strongly on its surface properties. For instance, hexagonal (111) Pt surfaces are 3–7-times more active than cubic (100) surfaces for aromatization reactions.[5] The reactivity and selectivity of nanoparticles can therefore be tuned by controlling the morphology because the exposed surfaces of the particles have distinct crystallographic planes depending on the shape.

A variety of Pt nanostructures, including polyhedra,[6] wires,[7] tubes,[8] dendritic structures,[9] and multipods[10] have been synthesized by regulating growth at specific surfaces or by templating methods. Amphiphilic polymers or surfactants typically stabilize high-energy surfaces of nanoparticles. However, chemical reactions can only occur effectively on catalytically "clean" nanoparticles when the reactants adsorb more strongly to the particle surface than the surface-stabilizing agents do.[11] When the interaction between the stabilizing agent and metal surface is too strong, the catalytic activity is greatly reduced. For instance, the carbonyl group of polyvinylpyrrolidone (PVP) or polyacrylate, which are the most widely used surface-regulating polymers in shaped-nanoparticle synthesis, interacts strongly with the platinum surface[12] and thus blocks a significant number of active sites. On the other hand, alkylammonium ions have been widely used in synthesizing Au nanoparticles,[13] and their interactions with Pt surfaces are considerably weaker than that of the carbonyl group. Therefore, this class of molecules could serve as ideal surface-stabilizing agents that can regulate the shape of nanoparticles while preserving catalytically active sites.

[*] H. Lee, S. E. Habas, S. Kweskin, D. Butcher, Prof. G. A. Somorjai, Prof. P. Yang
Department of Chemistry
University of California, Berkeley
Materials Science Division
Lawrence Berkeley National Laboratory
Berkeley, CA 94720 (USA)
Fax: (+1) 510-642-7301
E-mail: p_yang@uclink.berkeley.edu

[**] This work was supported by the Director, Office of Science, Office of Basic Energy Sciences, Chemical Sciences, Materials Sciences and Engineering Division of the U.S. Department of Energy under contract No. DE-AC02-05CH11231. We thank the National Center for Electron Microscopy for the use of their facilities.

Supporting Information for this article is available on the WWW under http://www.angewandte.org or from the author.

Interestingly, shape-control of platinum nanoparticles using alkylammonium ions has not been reported.

The addition of foreign metal ions is very effective for controlling morphology. Xia and co-workers, for example, have obtained multipods and nanowires by altering the reduction kinetics with Fe ions.[7a,14] We have also reported recently that highly uniform Pt cubes, cuboctahedra, and octahedra can be prepared by adding Ag ions prior to the reduction of the Pt precursor.[6c] The catalytic activity of these particles, however, is greatly reduced by the presence of Ag. As the amount of Ag is increased from the cubic to the octahedral samples, the reaction rate for ethylene hydrogenation decreases accordingly.[15] Therefore, shape-control of uniform Pt nanoparticles without the aid of foreign metal ions is highly desirable for catalytic applications.

Herein, we report the preparation of cuboctahedra, cubes, and porous Pt nanoparticles by varying the reduction method, as illustrated in Scheme 1. Near-monodisperse nanoparticles

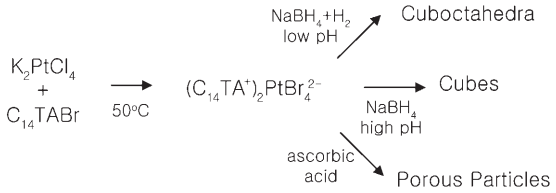

Scheme 1. Reduction of a metal–surfactant complex can be kinetically controlled to produce cuboctahedra, cubes, and porous particles.

are obtained in which tetradecyltrimethylammonium bromide ($C_{14}TABr$) is bound to the Pt surfaces. Potassium tetrachloroplatinate (K_2PtCl_4) forms a precipitate upon mixing with $C_{14}TABr$ in aqueous solution. After heating at 50 °C, the solution becomes clear pale yellow and then turns dark brown after reduction. The UV/Vis spectra show that after mixing with the surfactant the characteristic absorption of K_2PtCl_4 at 216 nm disappears and a new band appears at 271 nm (Supporting Information, Figure S1). It has been reported that $[PdCl_4]^{2-}$ ions interact with $C_{14}TABr$ to form the stoichiometric metal–surfactant complex $(C_{14}TA)_2PdBr_4$.[16] Likewise, the complex of $(C_{14}TA)_2PtBr_4$ is considered to be the real precursor during the reduction process.

To optimize the conditions for nanoparticle preparation various concentrations and ratios of K_2PtCl_4 and $C_{14}TABr$ were explored. Particle formation was observed over a broad range of reagent concentrations (20–200 mM $C_{14}TABr$ and 0.5–5 mM K_2PtCl_4) and ratios ($C_{14}TABr/K_2PtCl_4 = 25$–$400$). Generally, the size of the nanoparticles was found to increase as the concentration of the reagents and ratio of K_2PtCl_4 to $C_{14}TABr$ increased. Shape evolution of the nanoparticles from dendritic structures to faceted nanoparticles, such as cubes, was observed when sodium borohydride ($NaBH_4$) was used as the reducing agent. On the other hand, porous particles of various sizes dominated when the reducing agent was ascorbic acid. The reactant composition and the amount of reducing agent were finely tuned to 1) achieve a uniform distribution of size and shape, and 2) prepare particles of differing morphology within the same size range.

Figure 1 shows TEM and high-resolution (HR) TEM images of Pt nanoparticles with different morphologies.

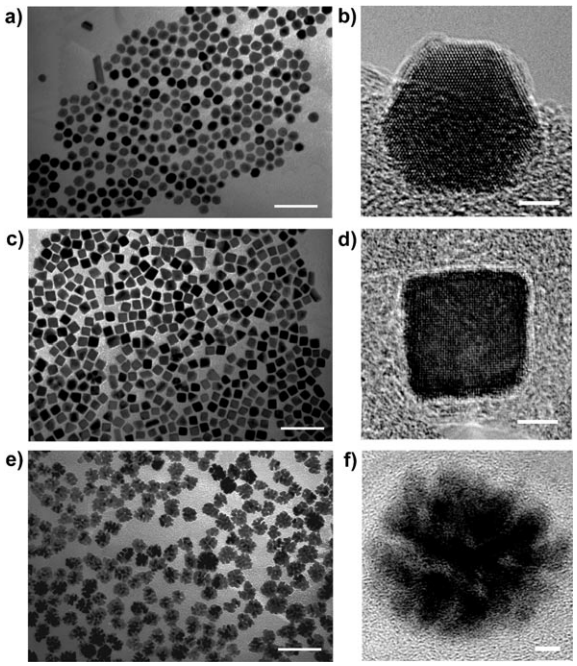

Figure 1. TEM images of a) cuboctahedra, c) cubes, and e) porous particles. HRTEM images of b) a cuboctahedron along the [111] zone axis, d) a cube along the [100] zone axis, and f) a porous particle. The scale bar is 50 nm in the TEM images and 3 nm in the HRTEM images.

Cuboctahedral particles (91 % cuboctahedra, 9 % spheres or irregular particles) with an average size of (12.6 ± 1.8) nm (vertex-to-vertex) were prepared from a solution of 150 mM $C_{14}TABr$ and 1.5 mM K_2PtCl_4 reduced with 7.5 mM $NaBH_4$ in a mild H_2 flow. Figure 1b provides a representative HRTEM image of a Pt cuboctahedron along the [111] zone axis. Threefold symmetry from the (111) surface on the top of the particle can clearly be seen. Cubic particles (73 % cubes, 5 % tetrahedra, 22 % irregular particles) with an average size of (13.4 ± 1.8) nm (diagonal) were prepared from a 100 mM $C_{14}TABr$ and 1 mM K_2PtCl_4 solution reduced with 30 mM $NaBH_4$. The excess $NaBH_4$ reacts vigorously with water to produce a large amount of H_2. The resulting pressure inside the reaction vessel was released by inserting a needle into the septum covering the reactor. The HRTEM image of a Pt cube along the [100] zone axis is shown in Figure 1 d (Figure S2 a of the Supporting Information provides an electron diffraction pattern for a single Pt cube along the [100] zone axis). Porous particles (100 % yield) were obtained from a solution containing 50 mM $C_{14}TABr$ and 2 mM K_2PtCl_4 reduced with 6 mM ascorbic acid. The average size was estimated as (19.3 ± 3.1) nm by measuring the longest axis. The HRTEM image of the porous particle in Figure 1 f clearly shows its porous nature. The BET surface area was determined to be 25 $m^2 g^{-1}$

based on nitrogen gas absorption and desorption isotherm measurements. Interestingly, a single porous particle exhibits an electron diffraction pattern characteristic of a single crystalline particle (Supporting Information, Figure S2b).

For the same concentrations of C_{14}TABr and K_2PtCl_4, the amount of $NaBH_4$ used for reduction has a significant impact on the resulting particle morphology. This effect is illustrated in Figure 2. Dendritic particles were obtained for 7.5 mM $NaBH_4$, cuboctahedra for 30 mM $NaBH_4$, and cubes for 45 mM $NaBH_4$. Higher concentrations of $NaBH_4$ gave particles with irregular shapes. Notably, the particle size does not differ significantly for 30, 45, and 60 mM $NaBH_4$ (Figures 2b, c and d). If the addition of $NaBH_4$ causes instantaneous nucleation, as reported,[13b] the final particle size should be smaller for larger amounts of $NaBH_4$ owing to the increased number of initial nucleates. Also, the color of the solution generally turned dark brown a couple of hours after the addition of $NaBH_4$, thus disproving the immediate nucleation. These observations suggest that the H_2 produced by reaction of $NaBH_4$ with water might be truly responsible for the final morphology of the Pt nanoparticles rather than $NaBH_4$. It has also been reported that hydrogen-based reduction proceeds by slow nucleation and fast autocatalytic surface growth, thereby enabling the preparation of nearly monodisperse metal (Ir) nanoclusters.[17] A control experiment in the absence of H_2 was conducted by removing the septum from the reaction vessel to allow the H_2 to escape. Rather than the faceted nanoparticles obtained in the presence of H_2, the majority of the product precipitated as bulk Pt. TEM analysis of the gray supernatant solution showed aggregated particulates. It is noteworthy that the cuboctahedral Pt nanoparticles shown in Figure 1a were prepared similarly to the particles shown in Figure 2a but passing additional H_2 through the reactor.

The production of H_2 by $NaBH_4$ is greatly accelerated by an increase in temperature.[18] In contrast to the majority of other syntheses, which proceed at room temperature, the reactions described herein are performed at 50 °C. On the other hand, in the absence of $NaBH_4$ when only an H_2 flow was used to reduce a solution of 150 mM C_{14}TABr and 1.5 mM K_2PtCl_4, nanoparticles with various shapes and sizes were obtained (Supporting Information, Figure S3). The production of H_2 in situ throughout the solution by $NaBH_4$ seems to be critical for the synthesis of uniform Pt nanoparticles.

During the reaction of $NaBH_4$ with water, the pH value increases as a result of the formation of the strongly basic metaborate ion.[18] In fact, the pH value increases to 9.41, 9.63, 9.77, and 9.97 after the reduction of solutions containing 7.5, 20, 30, and 40 mM $NaBH_4$, respectively (Figure 2). This pH change is believed to cause the distinct morphologies reported herein. When only H_2 was used as the reductant (Supporting Information, Figure S3), the pH value decreased to 2.51. To mimic the change in pH value observed with the addition of $NaBH_4$, NaOH was added to a reaction under the conditions described for cuboctahedral growth. Starting from the cuboctahedral shape shown in Figure 3a, more cubic particles appear as NaOH is added, as shown in Figure 3b (0.01 mM NaOH) and Figure 3c (1 mM NaOH). For 3 mM NaOH, only aggregated particulates were obtained. When an excess of NaOH is added (pH ≈ 12), no reduction occurs even after 24 h. Cubic nanoparticles could also be prepared by adding NaOH when the reactant solution was reduced only with H_2 gas (Supporting Information, Figure S4). A higher pH value was found to decrease the reduction rate, with slower reduction enabling selective growth on the (100) surfaces to produce cubic nanoparticles.

The catalytic activity was tested for ethylene hydrogenation on two-dimensional nanoparticle arrays prepared by the Langmuir–Blodgett technique. The activity of the Pt nano-

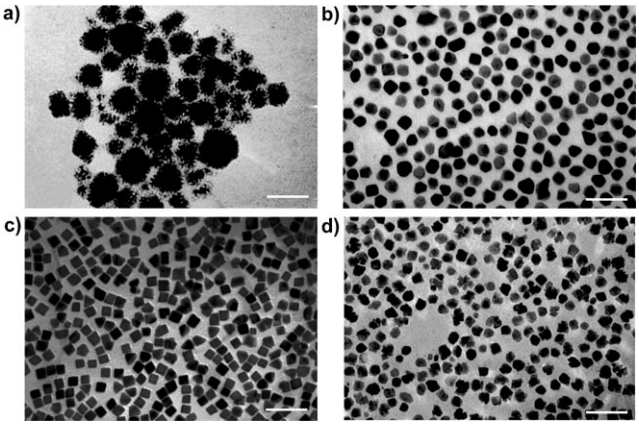

Figure 2. TEM images of Pt nanoparticles obtained by adding a) 7.5, b) 30, c) 45, and d) 60 mM $NaBH_4$ to a clear aqueous solution of 150 mM C_{14}TABr and 1.5 mM K_2PtCl_4. Shape evolution was clearly observed from dendritic nanostructures (a) to hexagonal (b), cubic (c), and irregular particles (d). The scale bar is 50 nm.

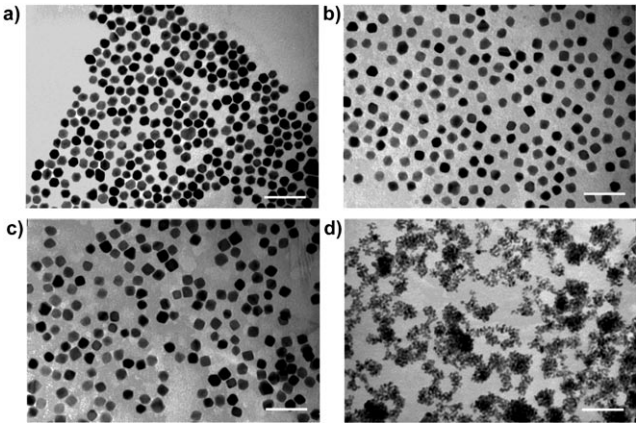

Figure 3. TEM images of Pt nanoparticles showing the effect of additional NaOH. The nanoparticles in a) were obtained from an aqueous solution with a composition of 150 mM C_{14}TABr, 1.5 mM K_2PtCl_4, and 7.5 mM $NaBH_4$ under mild H_2 flow. Addition of b) 0.01, c) 1, and d) 3 mM NaOH to a solution with the same composition as (a). More cubic nanoparticles were observed when NaOH was added, while an excess of NaOH produced only aggregated particulates. The scale bar is 50 nm.

particles synthesized in this work was compared with Pt nanoparticles prepared as reported previously.[6c] Cubes with an average size of 9.4 nm (diagonal) and cuboctahedra with an average size of 9.1 nm (vertex-to-vertex) were prepared using a polymeric capping agent (PVP) and Ag (1.1 and 11 mol%, respectively).[6c] The C_{14}TABr-capped Pt nanoparticles have much higher catalytic activity than PVP-capped Pt nanoparticles (Figure 4). At 373 K, the C_{14}TABr-capped

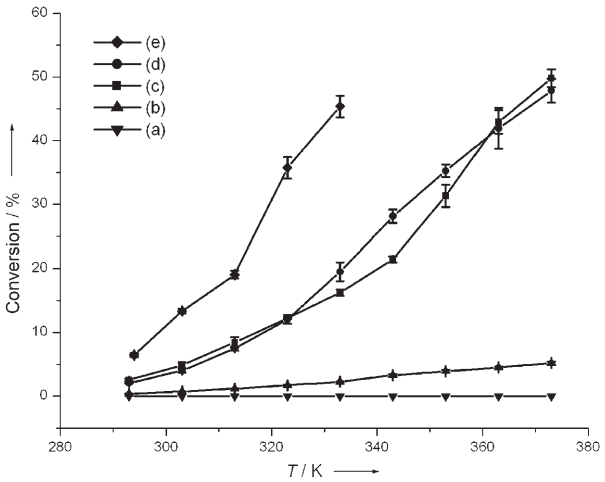

Figure 4. Comparison of catalytic activity for ethylene hydrogenation when using a) (▼) PVP-capped Pt cuboctahedra with 11 mol% Ag (9.1 nm, vertex-to-vertex), b) (▲) PVP-capped Pt cubes with 1.1 mol% Ag (9.4 nm, diagonal), c) (■) C_{14}TABr-capped Pt cubes (13.4 nm, diagonal), d) (●) C_{14}TABr-capped Pt cuboctahedra (12.6 nm, vertex-to-vertex), and e) (◆) C_{14}TABr-capped Pt porous particles (19.3 nm, longest axis). No treatment was performed to remove the capping agents.

cubes are about 10-times more active than the PVP-capped cubes. PVP-capped cuboctahedra prepared with 11 mol% Ag show no catalytic activity under these reaction conditions. The C_{14}TABr-capped porous nanoparticles have the highest activity for ethylene hydrogenation owing to their having a much larger surface area than the cubes or cuboctahedra.[19] The effect of different shapes on catalytic activity will be investigated in a future study.

In summary, cubic, cuboctahedral, and porous Pt nanoparticles have been prepared using tetradecyltrimethylammonium bromide as a surface-stabilizing reagent. The morphology was controlled by adjusting the reduction method. H_2 production in situ from $NaBH_4$ has enabled the synthesis of uniform nanoparticles. By changing the pH value, which contributes to controlling the reduction rate, shape evolution from cuboctahedra to cubes was observed. These nanoparticles, which are electrostatically capped with alkylammonium ions and shape-controlled without the aid of foreign metal ions, show superior catalytic activity to nanoparticles prepared with a polymeric stabilizing reagent and silver.

Experimental Section

In a typical synthesis, aqueous solutions of K_2PtCl_4 (Alfa Aesar, 99.9%) and C_{14}TABr (Aldrich, 99%) were mixed in a 20-mL vial at room temperature. The mixture was heated at 50°C for about 5 min until the solution became clear. The vial was capped with a rubber septum immediately after adding ice-cold $NaBH_4$ (Strem Chemicals, 98%) and the H_2 gas pressure inside the vial was released through a needle in the septum for 10 min. The needle was then removed and the solution was kept at 50°C for 6 h. When L-ascorbic acid (Aldrich, 99 + %) was used as the reducing agent the solution was kept at 70°C. The total volume of the solution was maintained at 10 mL. When necessary, H_2 gas was passed through the solution slowly for 5 min and then pressurized for 1 min without an exit needle. The product was centrifuged at 3000 rpm for 30 min. The supernatant solution was separated and centrifuged again at 12000 rpm for 10 min. The precipitate was collected and re-dispersed in 5 mL of deionized water by sonication.

UV/Vis absorption spectra were recorded with an Agilent 8453 UV/Vis system. TEM and HRTEM images were obtained with a Jeol 200CX microscope and a Philips CM200 microscope, respectively, operating at 200 kV, at the National Center for Electron Microscopy at the Lawrence Berkeley National Laboratory. The surface area was measured with a Quantachrome Autosorb-1 analyzer at 77 K using nitrogen as the adsorption gas. Before the measurement, degassing was conducted at 150°C for 48 h to remove possible moisture. The pH value was measured with a Mettler Toledo MP220 pH meter.

A special cell was constructed for ethylene hydrogenation studies under continuous gas-flow conditions. A silicon wafer with Pt nanoparticles deposited by the Langmuir–Blodgett (LB) technique was compressed against a rubber O-ring (16 mm I.D.) by tightening a Teflon block by two set screws. The reaction cell was connected to a stainless-steel gas manifold, which was equipped with mass flow controllers (MFC, Porter Instrument Company). The flow rate of C_2H_4 (AirGas, CP grade), H_2 (Praxair, UHP, 99.999%), and He (Praxair, UHP, 99.999%) was 1.0, 13.9, and 83.0 mL min^{-1}, respectively. The flow reactor was sampled periodically by gas chromatography (GC). The coverage of Pt nanoparticles on the substrate was examined and the conversion of ethylene into ethane was corrected by considering the different coverage for direct comparison of the LB samples.

Received: July 28, 2006
Published online: November 7, 2006

Keywords: heterogeneous catalysis · morphology control · nanostructures · platinum · surfactants

[1] a) F. Porta, M. Rossi, *J. Mol. Catal. A* **2003**, *204–205*, 553; b) H. Bonnemann, W. Brijoux, A. S. Tilling, K. Siepen, *Top. Catal.* **1997**, *4*, 217; c) N. Toshima, Y. Shiraishi, T. Teranishi, M. Miyake, T. Tominaga, H. Watanabe, W. Brijoux, H. Bonnemann, G. Schmid, *Appl. Organomet. Chem.* **2001**, *15*, 178.
[2] a) J. Prabhuram, X. Wang, C. L. Hui, I.-M. Hsing, *J. Phys. Chem. B* **2003**, *107*, 11057; b) Z. Chen, X. Qiu, B. Lu, S. Zhang, W. Zhu, L. Chen, *Electrochem. Commun.* **2005**, *7*, 593.
[3] L. Sun, D. V. Ca, J. A. Cox, *J. Solid State Electrochem.* **2005**, *9*, 816.
[4] A. Kolmakov, D. O. Klenov, Y. Lilach, S. Stemmer, M. Moskovits, *Nano Lett.* **2005**, *5*, 667.
[5] S. M. Davis, F. Zaera, G. A. Somorjai, *J. Catal.* **1984**, *85*, 206.
[6] a) T. S. Ahmadi, Z. L. Wang, A. Henglein, M. A. El-Sayed, *Chem. Mater.* **1996**, *8*, 1161; b) J. M. Petroski, A. L. Wang, T. C. Green, M. A. El-Sayed, *J. Phys. Chem. B* **1998**, *102*, 3316; c) H. Song, F. Kim, S. Connor, G. A. Somorjai, P. Yang, *J. Phys. Chem. B* **2005**, *109*, 188; d) T. Teranishi, R. Kurita, M. Miyake, *J. Inorg. Organomet. Polym.* **2000**, *10*, 145; e) A. Miyazaki, Y. Nakano, *Langmuir* **2000**, *16*, 7109; f) B. Veisz, L. Toth, D. Teschner, Z.

Paal, N. Gyorffy, U. Wild, R. Schlögl, *J. Mol. Catal. A* **2005**, *238*, 56.
[7] a) J. Chen, T. Herricks, M. Geissler, Y. Xia, *J. Am. Chem. Soc.* **2004**, *126*, 10854; b) X. Fu, Y. Wang, N. Wu, L. Gui, Y. Tang, *J. Mater. Chem.* **2003**, *13*, 1192.
[8] a) T. Kijima, T. Yoshimura, M. Uota, T. Ikeda, D. Fujikawa, S. Mouri, S. Uoyama, *Angew. Chem.* **2004**, *116*, 230; *Angew. Chem. Int. Ed.* **2004**, *43*, 228; b) B. Mayers, X. Jiang, D. Sunderland, B. Cattle, Y. Xia, *J. Am. Chem. Soc.* **2003**, *125*, 13364.
[9] a) Y. Song, Y. Yang, C. J. Medforth, E. Pereira, A. K. Singh, H. Xu, Y. Jiang, C. J. Brinker, F. van Swol, J. A. Shelnutt, *J. Am. Chem. Soc.* **2004**, *126*, 635; b) X. Zhong, Y. Feng, I. Lieberwirth, W. Knoll, *Chem. Mater.* **2006**, *18*, 2468; c) X. Teng, X. Liang, S. Maksimuk, H. Yang, *Small* **2006**, *2*, 249.
[10] X. Teng, H. Yang, *Nano Lett.* **2005**, *5*, 885.
[11] R. Narayanan, M. A. El-Sayed, *J. Phys. Chem. B* **2005**, *109*, 12663.
[12] Y. Borodko, S. E. Habas, M. Koebel, P. Yang, H. Frei, G. A. Somorjai, *J. Phys. Chem. B* **2006**, in press.
[13] a) J. Gao, C. M. Bender, C. J. Murphy, *Langmuir* **2003**, *19*, 9065; b) T. K. Sau, C. J. Murphy, *J. Am. Chem. Soc.* **2004**, *126*, 8648; c) F. Kim, J. H. Song, P. Yang, *J. Am. Chem. Soc.* **2002**, *124*, 14316; d) J. Perez-Juste, L. M. Liz-Marzan, S. Carnie, D. Y. C. Chan, P. Mulvaney, *Adv. Funct. Mater.* **2004**, *14*, 571.
[14] J. Chen, T. Herricks, Y. Xia, *Angew. Chem.* **2005**, *117*, 2645; *Angew. Chem. Int. Ed.* **2005**, *44*, 2589.
[15] R. M. Rioux, H. Song, M. Grass, S. Habas, K. Niesz, J. D. Hoefelmeyer, P. Yang, G. A. Somorjai, *Top. Catal.* **2006**, in press.
[16] B. Veisz, Z. Kiraly, *Langmuir* **2003**, *19*, 4817.
[17] M. A. Watzky, R. G. Finke, *J. Am. Chem. Soc.* **1997**, *119*, 10382.
[18] H. I. Schlesinger, H. C. Brown, A. E. Finholt, J. R. Gilbreath, H. R. Hoekstra, E. K. Hyde, *J. Am. Chem. Soc.* **1953**, *75*, 215.
[19] The porous nanoparticles showed little change in conversion at temperatures higher than 333 K, probably because of mass-transfer limitations at the given flow rate. The mass-transfer rate of C_2H_4 to the Pt surface is slower than the reaction rate of C_2H_4 on a Pt surface at high temperature, so the overall conversion is governed by the mass-transfer rate rather than by Pt catalyst activation. In fact, the conversion can be increased significantly by changing the flow rate. Catalyst deactivation was not observed.

